



# Microwave-assisted green synthesis of *Cassia alata*-mediated gold nanoparticles and evaluation of its antioxidant, anti-inflammatory, and antibacterial activities

Vania Clarissha Situmorang<sup>1</sup> · Sahrul Ramadhani<sup>1</sup> · Tia Okselni<sup>1</sup> · Marissa Angelina<sup>1</sup> · Rizna Triana Dewi<sup>1</sup> · Eldiza Puji Rahmi<sup>2</sup> · Hikmat Hikmat<sup>3</sup> · Melati Septiyanti<sup>3</sup> · Abdi Wira Septama<sup>1</sup>

Received: 4 February 2024 / Revised: 9 July 2024 / Accepted: 13 July 2024

© The Author(s), under exclusive licence to Springer-Verlag GmbH Germany, part of Springer Nature 2024

## Abstract

The increasing prevalence of antibiotic resistance has directed scientific inquiry toward the development of substitute therapies. Gold nanoparticles (AuNPs) have a variety of biological uses, including antioxidant, antibacterial, anticancer, and anti-inflammatory activities. Green synthesis was applied to the production of AuNPs using *Cassia alata* leaves (CAL) extract as a reducing agent. AuNPs were then characterized. The AuNPs were successfully synthesized as confirmed by the UV–Vis data with a maximum absorption peak at 534 nm. An average particle size distribution of  $63.647 \pm 1.334$  nm. These CAL-AuNPs were dominated by a spherical shape. X-ray diffraction studies indicated that the biosynthesized AuNP structures are crystallized. The intensity fluctuations of many peaks from Fourier-transform infrared spectroscopy analysis suggested the existence of bioconstituents responsible for capping and stability. Transmission electron microscopy (TEM) study revealed a spherical morphology for the AuNPs, agreeing with the findings obtained by dynamic light scattering (DLS). Following that, the biological performance of biomolecule-functionalized AuNPs was investigated. This study looked into the possible antioxidant, anti-inflammatory, and antibacterial benefits of produced AuNPs. CAL-AuNPs strongly inhibited the 1,1-diphenyl-2-picrylhydrazyl (DPPH) radicals with  $IC_{50}$  of 6.890  $\mu\text{g/mL}$ . A low CAL-AuNPs concentration of 50  $\mu\text{g/mL}$  highly suppressed protein denaturation (45.22%). CAL-AuNPs possessed antibacterial activity against *Staphylococcus aureus*, *Streptococcus pyogenes*, and *Bacillus subtilis* with MIC values in the range of 125 to 250  $\mu\text{g/mL}$ . In conclusion, green-synthesized AuNPs using *C. alata* leaf extract have great potential as antioxidant, anti-inflammatory, and antibacterial agents.

**Keywords** Antioxidant · Anti-inflammatory · Antibacterial · *Cassia alata* · Gold nanoparticle

## 1 Introduction

Nanotechnology involves the creation of material at nanoscale, ranging from 1 to 100 nm [1]. Amongst several types of nanomaterials, nanoparticles are attracting attention in various fields. Nanoparticle production is cheap and easy to perform, and their small size also facilitates drug delivery, thus maximizing the effectiveness of the treatment [2]. Several metals have reportedly been produced in nanoparticle form including gold nanoparticles (AuNPs) [3, 4]. The properties of AuNPs, such as having precise particle shapes and lengths, make AuNPs safer to use as drug delivery agents [5]. AuNPs can be synthesized by physical and chemical methods. The green synthesis method has recently become popular for synthesizing nanoparticles, as it offers several advantages, including eco-friendliness, low cost, and less

✉ Abdi Wira Septama  
abdi001@brin.go.id

<sup>1</sup> Research Center for Pharmaceutical Ingredients and Traditional Medicine, National Research and Innovation Agency (BRIN), Kawasan Sains Dan Teknologi (KST) Soekarno, Cibinong 16911, Indonesia

<sup>2</sup> Department of Pharmacy, Universitas Pembangunan Nasional Veteran Jakarta, Jalan RS Fatmawati, Jakarta 12450, Indonesia

<sup>3</sup> Research Center for Chemistry, National Research and Innovation Agency of Indonesia, Serpong 15314, Indonesia

toxicity, due to the utilization of non-toxic materials, such as fungi, plants, and bacteria [4–7]. The utilization of plants in the green synthesis of AuNPs is related to their secondary metabolite compounds, such as polyphenols, flavonoids, terpenoids, alkaloids, and amino acids. These compounds act as reducing and capping agents in the production of AuNPs, contributing to their characteristics and stability in green synthesis [8–10]. This research seeks to contribute to advancements in this field by focusing on the green synthesis of AuNPs using plant extract as a sustainable option.

The green synthesis of AuNPs has been achieved using various plant extracts, including *Simarouba glauca* leaf, *Targetes erecta* L. flowers, *Hibiscus sabdariffa* L. flowers, *Ziziphus zizyphus* leaf, and *Hygrophila spinosa* T. Anders [11–14]. A previous literature study also presented that AuNPs mediated by plants of *Garcinia mangostana*, *Couroupita guianensis*, *Acanthopanax sessiliflorus*, *Sporosarcina koreensis*, and *Sargassum swartzii* had different physical properties such as morphology and size, resulting in the differences of their biological properties [15]. One of the medicinal plants that can be used to synthesize AuNP is *Cassia alata*. This plant is a member of the Fabaceae family [16]. *C. alata* has been reported to have several pharmacological activities, including antimicrobial, antioxidant, and anti-inflammatory activities [17]. Another study also reported that *C. alata* extract had antibacterial activity against *Klebsiella pneumoniae*, *Staphylococcus aureus*, *Proteus mirabilis*, and *Escherichia coli* [18]. These pharmacological activities are associated with the phytochemicals, such as alkaloids, flavonoids, terpenoids, saponins, and tannins [19].

In the case of antibiotic resistance, bacterial infections are gradually growing resistant to a wide range of medications. Antibiotics are no longer useful for preventing or treating infections. To tackle resistant microbes, novel antimicrobial drugs with unique mechanisms of action are urgently needed. Nanotechnology presents a potential substitute in an era marked by growing worries about antibiotic-resistant bacteria, the emergence of infectious diseases, and the expanding need for potent antimicrobial treatments [20]. AuNPs are excellent prospects for new, long-lasting antibacterial medicines due to their outstanding antibacterial qualities against a variety of microorganisms. Besides that, AuNPs also exhibited several biological properties such as anti-inflammatory, antioxidant, and anti-tyrosinase properties [21].

Despite the growing interest in the green synthesis of AuNPs, there is a lack of research on the use of *C. alata* extract for the synthesis of AuNPs and its potential biological activities. The aim of this work is to synthesize AuNPs using *C. alata* leaf extract in a cost-effective and environmentally benign method. In the subsequent sections, experimental procedures for the synthesis will be discussed,

followed by assessments of their properties and antibacterial, antioxidant, and anti-inflammatory potential applications.

## 2 Materials and methods

### 2.1 Materials

Hydrogen tetrachlorocuprate (III) trihydrate, [HAuCl<sub>4</sub>·3H<sub>2</sub>O (99.9%)], 2,2 diphenyl-1-picrylhydrazyl (DPPH), quercetin, bovine serum albumin, sodium diclofenac, and tetracycline were purchased from Sigma-Aldrich, UK. *Staphylococcus aureus*, *Streptococcus pyogenes*, and *Bacillus subtilis* were provided by the Research Centre for Pharmaceutical Ingredients and Traditional Medicine. Brain Heart Infusion (BHI) broth and 0.5 McFarland were obtained from Himedia. Dimethyl sulfoxide (DMSO) was purchased from Vivantis. Methanol and ethanol were purchased from J.T. Baker, USA. Acetic acid and sodium chloride were purchased from Merck, Germany.

### 2.2 Collection of *Cassia alata* leaves and preparation of ethanolic extract

The fresh *C. alata* leaves were collected from Indonesia. Ethanolic extract of CAL was prepared using maceration as described by the previous method [19]. In brief, *C. alata* leaves were dried and ground using a blender to get the powder. The powder was soaked with 70% ethanol at a ratio of 1:5 (ratio of powder and solvent) and stirred by a shaker at 110 rpm for 18 h. The extraction process was carried out repeatedly until the color of the macerate matched the color of the solvent. Afterward, the extract was evaporated using a vacuum evaporator at 50 °C, resulting in a thick and concentrated extract.

### 2.3 Chemical compound determination by liquid chromatography with tandem mass spectrometry (LCMS/MS)

Quadrupole Time of Flight Liquid Chromatography-Mass Spectrometry (QTOF LCMS/MS) was used to identify the chemical components of the CAL extract. A 1.7 m 2.1 × 100 mm column with an ACQUITY UPLC BEH C8 is used for this measurement. Solvents A and B (0.1% formic acid in H<sub>2</sub>O and 0.1% formic acid in acetonitrile) were used as a binary mobile phase. 0.3 mL/min was the flow rate. Data were determined by the UNIFI program.

### 2.4 Green synthesis of gold nanoparticles (AuNPs)

HAuCl<sub>4</sub> was used as the gold precursor, and CAL extract was used as the reducing agent. The solution of HAuCl<sub>4</sub> was

added (19 mL, 0.1 mM) to an Erlenmeyer flask containing 1 mL of *C. alata* leaf extract (10 mg/mL, dissolved in distilled water). Microwave irradiation of 900 W was applied to the reaction mixture for 30 s per cycle. The *C. alata* leaves-gold nanoparticles (CAL-AuNPs) were formed through two microwave cycles, as evidenced by the change in color from yellowish to purple [22]. After the reaction time, the solution was centrifuged for 2 h at 60,000 rpm to obtain the pellets. The purified pellets of CAL-AuNPs were dried at 45 °C in a vacuum oven.

## 2.5 Characterization of CAL-AuNPs

The CAL-AuNPs were identified by a UV–visible spectrophotometer (Agilent Technologies G6860A Cary 60 UV–Vis) at 200–800 nm. Fourier-transform infrared spectroscopy (FTIR) was recorded using a Bruker Tensor II series spectrometer. FTIR spectra were recorded in the range of 4000–500  $\text{cm}^{-1}$  with a resolution of 4  $\text{cm}^{-1}$ . X-ray diffraction (XRD) analysis was conducted to evaluate the crystal structure using the X-ray diffractometer of Malvern PANalytical, AERIS model (Panalytical, Malvern, UK). The measurements were performed using nickel-filtered Cu K $\alpha$  radiation ( $\lambda = 1.5406 \text{ \AA}$ ) generated with a current of 15 mA and a voltage of 40 kV. XRD patterns were recorded from 5 to 80 °C with a scanning speed of 5°/min. An instrument of Jeol JIB-4610F equipped with a Schottky electron gun was used to observe the surface morphology through field emission scanning electron microscopy (FE-SEM) (Jeol JIB-4610F) and elemental composition through X-ray spectroscopy (EDX) (PANalytical AERIS model). A transmission electron microscope (TEM) (Tecnai G2 20 S-Twin instrument) was used to analyze the shape and size of CAL-AuNPs, in which the size was calculated using ImageJ software. The hydrodynamic particle size was also determined using dynamic light scattering (DLS) (Horiba SZ-100). Zeta potential analysis was used to evaluate the stability of nanoparticles using laser Doppler electrophoresis (nanoPartica SZ-100V2 Series, Horiba Scientific).

## 2.6 Antioxidant activity assay

The free radical scavenging activity was investigated by the 1,1-diphenyl-2-picrylhydrazyl (DPPH) method following the previous studies [23]. The samples at various concentrations in methanol solvent (300  $\mu\text{L}$ ) were prepared and added with 300  $\mu\text{L}$  of 0.2 mM DPPH dissolved in methanol. The mixture was incubated at room temperature in complete darkness for 30 min. The absorbance was measured at 517 nm. Quercetin was used as the control positive, and the methanol solvent was used as the blank. The inhibitory activity (%) was calculated using the following equation:

$$\% \text{ Inhibition} = \frac{A_{\text{control}} - A_{\text{sample}}}{A_{\text{control}}} \times 100$$

where  $A_{\text{control}}$  is the absorbance of the mixture of blank and DPPH solution and  $A_{\text{sample}}$  is the absorbance of the mixture of sample and DPPH. The  $\text{IC}_{50}$  value was calculated using the linear regression equation by plotting the regression curve of percentage scavenged versus concentration for each sample [24]. Further calculation was conducted by determining the antioxidant activity index (AAI) through the equation below:

$$\text{AAI} = \frac{\text{final concentration of DPPH radicals } (\mu\text{g/mL})}{\text{IC}_{50} (\mu\text{g/mL})}$$

## 2.7 Anti-inflammatory activity assay

The anti-inflammatory activity of CAL-AuNPs was evaluated using a protein denaturation assay of a previous study [25]. Briefly, the reaction mixture was prepared by adding 2850  $\mu\text{L}$  of 0.2% bovine serum albumin (BSA) solution (dissolved in 0.2 M Tris–acetate buffer, pH 6.5) and 150  $\mu\text{L}$  of samples. The reaction mixture was incubated at room temperature for 15 min, heated in a water bath at 70 °C for 5 min, and cooled at room temperature for 20 min. Methanol was used as the negative control. The absorbance was measured at 660 nm. The inhibition percentage of denaturation was calculated using the following equation:

$$\% \text{ Inhibition} = \left[ 1 - \frac{(A_{\text{sample}} - A_{\text{control}})}{A_{\text{control}}} \right] \times 100$$

$A_{\text{control}}$  is the absorbance of the negative control and  $A_{\text{sample}}$  is the absorbance of the samples. In addition, the activity index was also applied in order to understand the relationship between the sample and the anti-inflammatory standard. The calculation was obtained from the following equation and expressed as percent.

$$\text{AI}(\%) = \frac{\text{inhibition percentage of sample}}{\text{inhibition percentage of sodium diclofenac}} \times 100$$

## 2.8 Antibacterial activity assay

The slightly modified broth microdilution method (NCCLS, 2008) was used to evaluate the antibacterial activity against *Staphylococcus aureus*, *Streptococcus pyogenes*, and *Bacillus subtilis* [26]. All examined bacterium was cultured for 24 h at 37 °C on BHI agar. A few bacterial colonies were mixed with normal saline solution (NaCl 0.85%) to create the inocula, and the suspension's turbidity was adjusted to match the standard

0.5 McFarland solution, which was stated to be equal to  $1 \times 10^8$  CFU/mL. To get the suspension to contain about  $1 \times 10^6$  CFU/mL, it was diluted (1:100) with sterile normal saline solution. Next, to obtain the desired final concentration, each sample was first dissolved in DMSO and then diluted with BHI broth. A 96-well plate was used to prepare twofold dilutions. After being introduced to each well, the bacterial suspensions ( $1 \times 10^6$  CFU/mL) were incubated for 24 h at 37 °C. The lowest sample concentration that inhibited bacterial growth was found to be the MIC value.

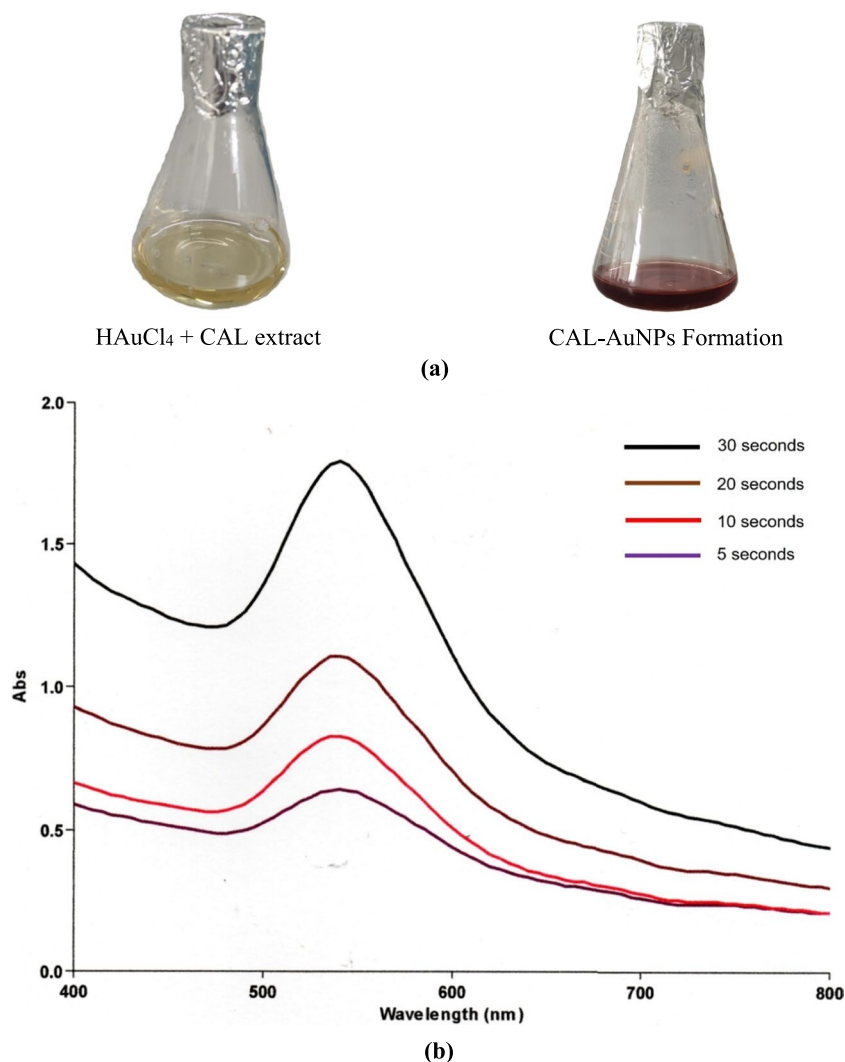
## 2.9 Statistical analysis

Each experiment was conducted in triplicate and the results are expressed as mean  $\pm$  standard deviation. The data was analyzed using Microsoft Excel Software.

## 3 Results and discussion

The gold nanoparticles (AuNPs) were synthesized greenly using the Indonesian medicinal plant of *C. alata*. The leaves of *C. alata* acted as a reducing agent of the  $\text{HAuCl}_4$  solution assisted by microwave irradiation to optimize the reaction. The formation of CAL-AuNPs was indicated by a final change in purple color (Fig. 1a). The final reacted solution was further confirmed by UV–Vis spectra, with a maximum peak at 534 nm (Fig. 1b). The color change is caused by surface plasmon resonance (SPR), which excites all free electrons within the conduction band. A previous study reported that the microwave-aided method yields *Ganoderma lucidum* AuNPs with smaller size in a shorter duration of time compared to the conventional method [27]. Similarly, research indicates that AuNPs synthesized using plum waste extract and licorice root extract exhibit an absorption peak at 540 nm [28, 29]. In addition, *Capsicum annum* fruit

**Fig. 1** The synthesized CAL-AuNP identification, **a** the color change and **b** UV–Vis spectrum for surface plasmon resonance (SPR)



and *Brassica rapa* var. *pekinensis* leaf extracts were used as bio-reducers for gold nanoparticle synthesis and exhibited an absorption peak at 540 nm [30, 31].

The potential secondary metabolites that reduced the metal ions and thus formed AuNPs were then identified using Fourier-transform infrared (FTIR) spectroscopy. The IR spectrum of *C. alata* leaves and CAL-AuNPs (Fig. 2) exhibited bands at 3264.48 and 3232.24  $\text{cm}^{-1}$  conforming O–H bonds in alcoholic or phenolic groups, as well as at 2927.26, 2918.58, and 2850.02  $\text{cm}^{-1}$  corresponding to C–H stretching alkanes. Bands at 1513.87, 1513.18, and 1443.65  $\text{cm}^{-1}$  were the stretching vibrations of C=C aromatics. Intense peaks at 1041.29 and 1055.91  $\text{cm}^{-1}$  corresponded to the C–O stretch of alcohols or ethers. All of the observed IR spectra were compared with previous studies [32, 33]. In general, the IR spectrum of CAL-AuNPs and *C. alata* leaves showed similar bands indicating that the compounds of *C. alata* leaves were capped on the surface of AuNPs, resulting in improving the CAL-AuNPs properties, such as the stability. As shown in Table 1, the plant extract contains various compounds such as 5,7,2',5'-tetrahydroxy-flavone, daturameteline I, kaempferol-3,7-diglucoside, 21-o-methyl toosendanopentaol, and 3,3',4,5'-tetramethoxy-trans-stilbene. *C. alata* leaf extract had constituents with the chemical structures of alcoholic, phenolic, alkane, aromatic, and carbonyl. Chemical compounds contained in *C. alata* leaf extract work as a bio-reductor in the formation of AuNPs, by converting  $\text{Au}^{3+}$  to  $\text{Au}^0$ . These organic compounds may be essential for the biosynthesis of AuNPs because of their capacity to function as reducing and capping agents for silver ions, which helps to stabilize AuNPs and inhibit aggregation (Fig. 3). Plant secondary metabolites for the bioreduction of  $\text{Au}^{3+}$  to  $\text{Au}^0$  and their concentration can affect the green-produced AuNPs' size, structure, and reaction

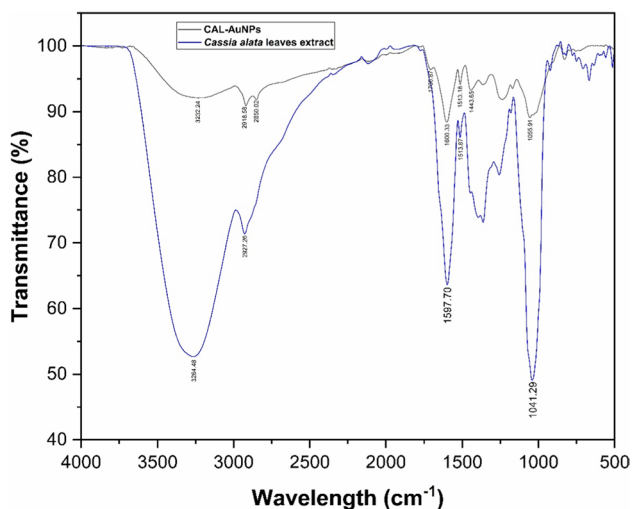


Fig. 2 FTIR spectra of *C. alata* leaves and CAL-AuNPs

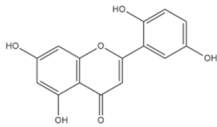
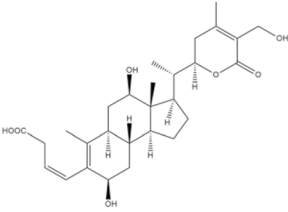
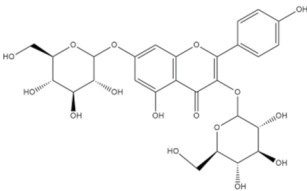
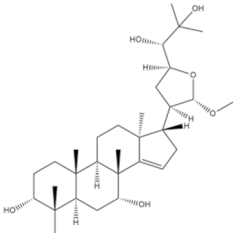
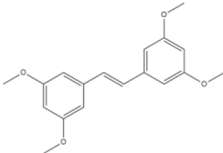
kinetics. The extract from the leaves of *C. alata* functions as a bio-reductor, converting gold ions ( $\text{Au}^{3+}$ ) into gold atoms ( $\text{Au}^0$ ), which are subsequently grouped to form colloidal AuNPs [34, 35].

The physical properties of CAL-AuNPs were identified through several measurements. The crystallographic nature of CAL-AuNPs was evaluated by X-ray diffraction studies. The result is presented in Fig. 4a. The XRD patterns of CAL-AuNPs presented four major diffraction peaks at  $2\theta$  values. As shown in the XRD spectrum (Fig. 3a), the four major diffraction peaks at  $2\theta$  values were observed at  $38.361^\circ$ ,  $44.311^\circ$ ,  $64.935^\circ$ , and  $77.632^\circ$ , corresponding to the (111), (200), (220), and (311) planes, respectively. Those peaks represented the face center cubic (FCC) crystal lattice of gold (Au). The XRD pattern of the CAL-AuNPs was compared to the Joint Committee on Powder Diffraction Standards (JCPDS) data No. 04–0748 to identify the crystal structure and phase of the nanoparticles [36]. This result was consistent with a number of studies. *Passiflora ligularis*-AuNPs exhibited an XRD pattern with diffraction angles of  $38.1^\circ$ ,  $44.51^\circ$ ,  $64.61^\circ$ , and  $77.82^\circ$ . Another study also revealed that using *Albizia lebbek* as a reducing agent in AuNP synthesis resulted in diffraction peaks at  $2\theta = 38.18^\circ$  (111),  $44.38^\circ$  (200), and  $66.57^\circ$  (220) [37, 38].

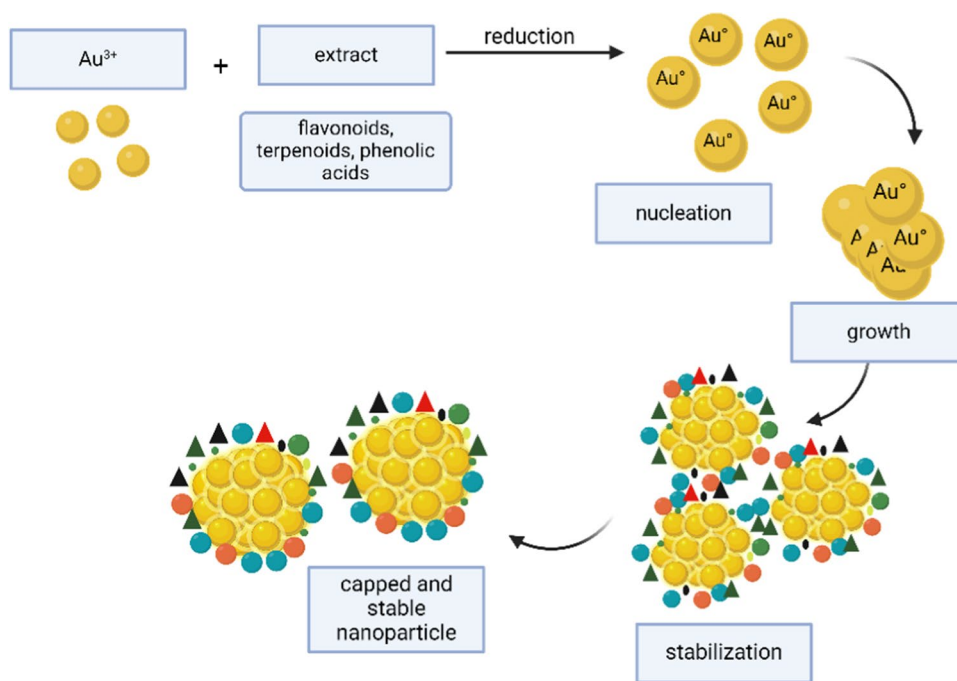
Furthermore, the surface morphology was measured by the FE-SEM. As shown in Fig. 4b, the illustration of the spherical shape of CAL-AuNPs was displayed indistinctly. The elemental composition of CAL-AuNPs was determined through EDX analysis. The spectra that are obtained show peaks that correspond to the elemental composition of the material. The components present in the reaction media were to be identified by means of the analysis of AuNPs, which were produced using *C. alata* leaf extract. These components may contribute to the conversion of Au ions into AuNPs. The EDX spectrum showed a strong Au signal with weak signals of C and O (Fig. 4c). These signals are probably caused by biomolecules that are attached to the surface of the nanoparticle. This discovery validates the presence of Au in the reaction media and implies that *C. alata* leaf extract, a useful bio-reductant for biosynthesis, played an important role in the synthesis of AuNPs.

TEM illustration was used to re-confirm the spherical form of the CAL-AuNPs. As shown in Fig. 5a, the CAL-AuNPs were clearly confirmed in spherical as the predominant shape. In addition, the study revealed the presence of triangular, diamond, and rectangular shapes. Several factors could be attributed to this discovery, such as the concentration of gold precursor and the volume and concentration of plant extracts, as well as the constituents of the plants acting as reducing agents [39, 40]. Secondary metabolites in plant extracts indirectly affected the shaping process of AuNPs, resulting in different shapes of nanoparticles. Furthermore, a number of studies reported that flavonoids and phenolic

**Table 1** LCMS/MS analysis of *Cassia alata* leaf extract

Structure	Name	RT [min]	Formula	Molecular Weight
	5,7,2',5'- Tetrahydroxy-flavone	8.82	C <sub>15</sub> H <sub>10</sub> O <sub>9</sub>	286.05
	Daturameteline I	10.86	C <sub>34</sub> H <sub>48</sub> O <sub>10</sub>	620.31
	Kaempferol- 3,7- diglucoside	5.48	C <sub>27</sub> H <sub>30</sub> O <sub>16</sub>	610.16
	21-o-methyl toosendanopentaol	10.62	C <sub>31</sub> H <sub>52</sub> O <sub>6</sub>	520.38
	3,3',4,5'-tetramethoxy-trans-stilbene	7.44	C <sub>14</sub> H <sub>12</sub> O <sub>4</sub>	300.14

**Fig. 3** The mechanism of the extract involved nanoparticle synthesis



compounds contained in the extract of *Hygrophila spinosa* T. Anders and *Elaeis guineensis* leaves participated in the fabrication of AuNPs in a spherical shape [14, 41]. In addition, Fig. 5b shows the particle size distribution of CAL-AuNPs with an average particle diameter of  $63.647 \pm 1.334$  nm. As the shape variation, the size of the particles was also affected by the extract volume and concentrations of the extract and precursor salt. Earlier study revealed that increasing the volume and concentration of *Aloysia triphylla* extract along with high precursor salt concentration produced the AuNPs with a size ranging from 40 to 60 nm [42]. Another study also reported that the high concentration of caffeic acid as a reducing agent produced a smaller size of AuNPs [43].

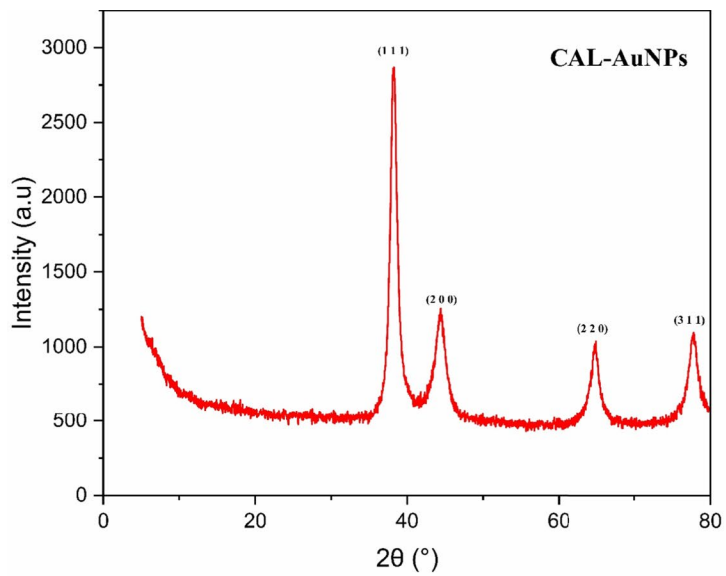
The hydrodynamic diameter of CAL-AuNPs was determined by DLS analysis. As shown in Fig. 5c, the CAL-AuNPs had an average particle size of  $78.3 \pm 3.1$  nm with a polydispersity index (PDI) of 0.397. The higher particle diameter of CAL-AuNPs was found through DLS than TEM analysis. This phenomenon was assumed due to the formation of particle aggregation because of the high nanoparticle concentration in the tested sample [44]. Moreover, our study showed that CAL-AuNPs had lower PDI value than the AuNPs mediated by *Sargassum tenerrimum* (PDI, 0.412) and *Turbinaria conoides* (PDI, 0.521). PDI value is associated with the homogeneity of the particles, in which a higher degree of homogeneity in the synthesized particles is indicated by a lower PDI value. PDI values above 0.7 show a broad particle size distribution profile [45, 46].

The surface charge and stability of CAL-AuNPs were evaluated by zeta potential analysis ( $\zeta$ ). It affects the toxicity and interaction between nanoparticles and cellular

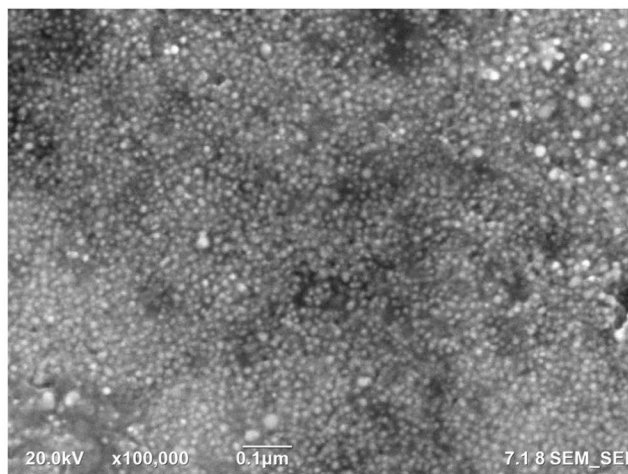
membranes. As shown in Fig. 6, the average zeta potential of CAL-AuNPs was  $-17.4$  mV indicating a negative surface charge. This zeta potential was classified as moderately stable [47]. Our finding was similar to the synthesized AuNPs mediated by *Rhodiola rosea* rhizome extracts ( $\zeta$ ,  $-18.1$  mV) and *Ligustrum vulgare* berries ( $\zeta$ ,  $-18.3$  mV) [48, 49]. The type of plant used in the synthesis of AuNPs can affect zeta potential. A previous study reported that plants with high antioxidant capacity tended to have a negative zeta potential value of AuNPs [50].

The antioxidant capabilities of AuNPs were examined using the simple and effective DPPH radical scavenging test method. Excess free radicals can collect in the body and create oxidative stress, which can damage healthy cells. As shown in Table 2, the antioxidant activity of the tested sample was in the order of *C. alata* leaves < CAL-AuNPs < quercetin. In consideration of their AAI value, *C. alata* leaf extract was categorized as having strong activity, whereas the CAL-AuNPs and the positive control of quercetin had very strong activity, as classified by [51]. Due to the ability to scavenge free radicals and support the body's defense mechanism against oxidative damage brought on by free radicals, antioxidants are vital to human health. Especially when made using biological or green synthesis procedures, researchers have found that AuNPs have a strong antioxidant potential to prevent oxidative damage [52, 53]. This distinct antioxidant activity might relate to the bioactive compounds of the plants used in synthesizing the AuNPs. Bioactive compounds, such as flavonoids and phenolic compounds, affect the antioxidant activity of extracts. Flavonoids donate hydrogen or electrons onto free

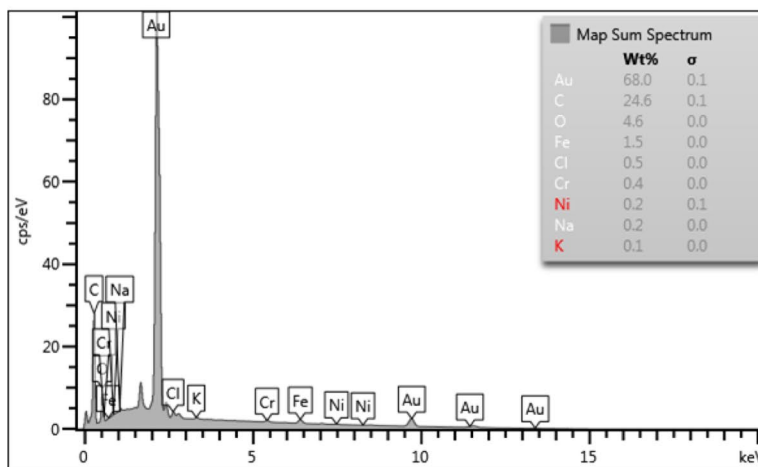
**Fig. 4** Characterization of CAL-AuNPs, a XRD pattern, b FE-SEM images, and c EDX mapping and spectrum



(a)



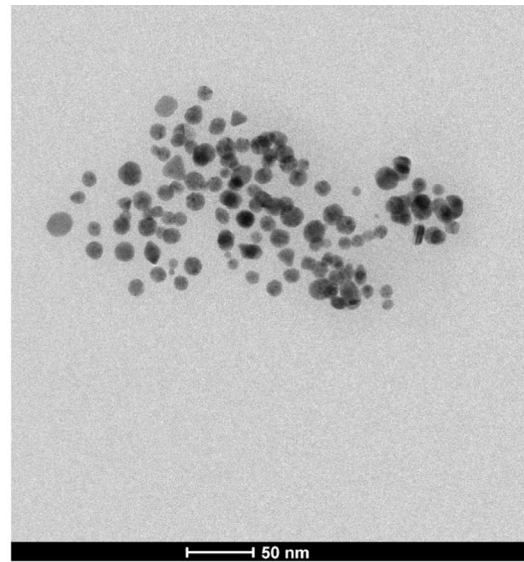
(b)



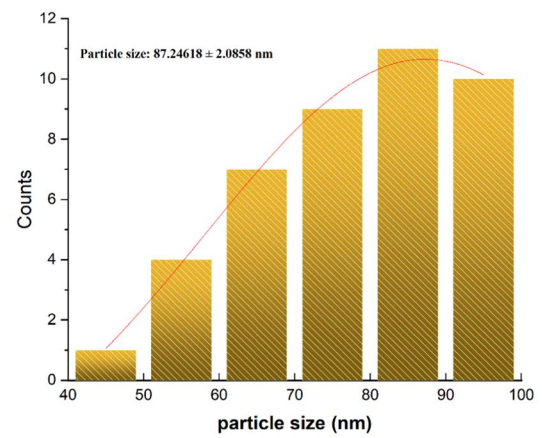
(c)



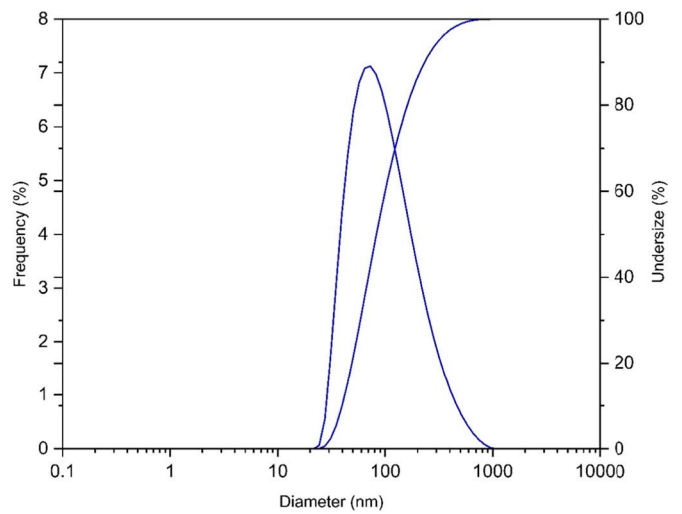
**Fig. 5** Particle size determinations of CAL-AuNPs, **a** TEM image, **b** particle size distribution graph calculated by ImageJ software, **c** hydrodynamic particle diameter by DLS



(a)



(b)



(c)

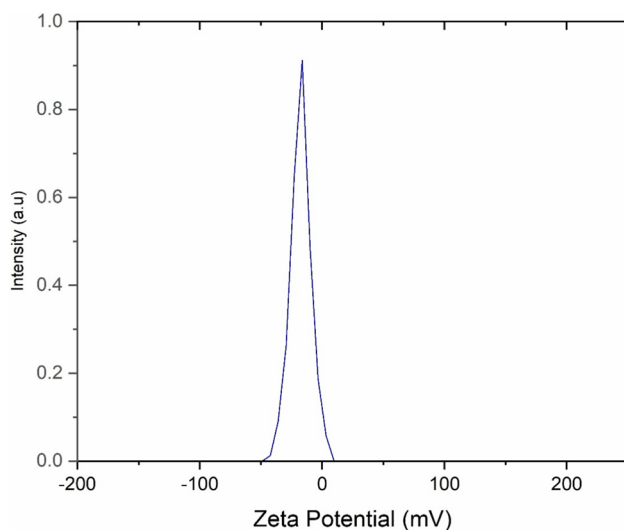


**Fig. 6** Zeta potential of CAL-AuNPs

**Table 2** The antioxidant activity of *Cassia alata* leaf extract, gold nanoparticles, and quercetin

Samples	IC <sub>50</sub> ± SD (µg/mL)	AAI
<i>Cassia alata</i> leaf extract	30.185 ± 0.485	1.307 ± 0.021
CAL-AuNPs	6.890 ± 0.167	5.726 ± 0.141
Quercetin*	2.835 ± 0.090	13.916 ± 0.449

The value was expressed as average ± standard deviation ( $n=3$ ) and the asterisk (\*) symbol indicated the control positive

radicals, which are responsible for the stability of radical compounds. Furthermore, benzene rings and the number of hydroxyl groups in phenolic compounds affect antioxidant activity [54]. Thus, it can be inferred that the presence of phenolic compounds and flavonoids enhances the antioxidant activity of CAL-AuNPs. The CAL-AuNPs had higher antioxidant activity than other AuNPs indicated by a low IC<sub>50</sub> value (6.890 µg/mL). This value was much lower than other AuNPs synthesized by *Mangifera indica* (IC<sub>50</sub> of 256 µg/mL) [55], *Citrus limetta* Risso (IC<sub>50</sub> value of 51.84 µg/mL) [56], *Kaempferia parviflora* rhizome (IC<sub>50</sub> value of 94.5 µg/mL) [57], and *Azadirachta indica* blossom (IC<sub>50</sub> value of 69.77 µg/mL) [58]. Furthermore, a previous study performed that the AuNPs exhibited higher DPPH radical scavenging activity than other metallic nanoparticles of AgNPs with the IC<sub>50</sub> value of 20 and 100 µg/mL, respectively [59].

The anti-inflammatory activity was investigated by an in vitro assay through the suppressing protein denaturation properties of the CAL-AuNPs and *C. alata* leaves. Protein denaturation occurs when proteins lose their tertiary and secondary structures due to external stress. Denaturation causes most biological proteins to lose their function. Compounds

preventing denaturation by more than 20% throughout concentration ranges were deemed anti-inflammatory [25]. As shown in Table 3, the anti-inflammatory activity of the tested sample was in the order of *C. alata* leaves < CAL-AuNPs < sodium diclofenac. The calculation of the activity index revealed that the anti-inflammatory activity of CAL-AuNPs was twice as high as that of *C. alata* leaves, with respective percentage values of 49.31% and 23.89%. This finding was supported by a previous study [60]. They found that AuNPs mediated by *Commiphora wightii* greatly inhibited protein denaturation with the IC<sub>50</sub> value of 87.85 µg/mL. Another study also performed the anti-inflammatory effect of AuNPs through the in vitro assay of human red blood cell membrane stabilization method and found that AuNPs effectively inhibited the heat-induced hemolysis with a percentage of 94% at 25 µg/mL [61].

In recent years, nanoparticles have drawn interest as a fascinating antibiotic substitution strategy and have shown considerable promise in combating bacterial multidrug resistance in human infections. AuNPs have many methods of action to kill bacteria, unlike antibiotics, which reduce the likelihood of bacterial resistance. As a result, AuNPs represent a novel class of antibacterial agents. The antibacterial properties of CAL-AuNPs were examined in this work against opportunistic pathogenic microorganisms. Based on broth microdilution, AuNPs exhibited antibacterial activity against *S. aureus*, *S. pyogenes*, and *B. subtilis* with MIC values of 62.5, 62.5, and 125 µg/mL, respectively (Table 4). However, these AuNPs did not show an antibacterial effect against *E. coli*. According to the results, the antibacterial activity of AuNPs was higher compared to *C. alata* leaf extracts. Utilization of plant extracts in green-synthesized AuNPs enhanced the antibacterial activity of AuNPs compared to plant extracts. As reported by [62], AuNPs mediated by *Sambucus wightiana* had high antibacterial activity against *E. coli*, *Salmonella enteritidis*, *Salmonella typhi*, and *S. epidermis* compared to *S. wightiana* extract. Synthesis method of AuNPs is one of the factors that affect the antibacterial activity of AuNPs. Numerous studies had suggested that particle size and shape also affected the antibacterial activity of green-synthesized AuNPs. The AuNPs with a smaller size of 7 nm showed good antibacterial activity against *S. aureus*, which enhanced the penetration of AuNPs

**Table 3** Anti-inflammatory activity using protein denaturation assay

Samples	Concentration (µg/mL)	% Inhibition ± SD
Sodium diclofenac*	50	91.707 ± 0.79
CAL-AuNPs	50	45.225 ± 2.70
<i>Cassia alata</i> leaf extract	50	21.905 ± 0.10

The value was expressed as average ± standard deviation ( $n=3$ ) and the asterisk (\*) symbol indicated the control positive

**Table 4** Antibacterial activity against *Staphylococcus aureus*, *Streptococcus pyogenes*, and *Bacillus subtilis*

Bacteria	Tetracycline*		CAL-AuNPs		<i>Cassia alata</i> leaf extract	
	MIC ( $\mu\text{g/mL}$ )	MBC ( $\mu\text{g/mL}$ )	MIC ( $\mu\text{g/mL}$ )	MBC ( $\mu\text{g/mL}$ )	MIC ( $\mu\text{g/mL}$ )	MBC ( $\mu\text{g/mL}$ )
<i>Staphylococcus aureus</i>	6.25	12.5	62.5	125	250	500
<i>Streptococcus pyogenes</i>	6.25	12.5	62.5	125	250	500
<i>Bacillus subtilis</i>	12.5	12.5	125	250	500	500
<i>Escherichia coli</i>	12.5	12.5	500	500	NA	NA

The asterisk (\*) symbol indicates the control positive

into bacterial cells [63, 64]. It has been reported that high surface-to-volume ratios are primarily responsible for antibacterial activity, and AuNPs' small size makes it easier for them to enter cell walls and membranes. Aggregating AuNPs on the cell surface can lead to pits, fissures, and pores that disrupt the permeability of the membrane [65]. Although the precise mechanism of the antibacterial action of AuNPs is not fully understood, however, some mechanisms of action have been suggested (Fig. 7). According to other research, there is no need for the redox syndrome to be connected to elevated ROS concentrations. It might have to do with AuNPs directly injuring the GPx enzyme, which aggravates oxidative cell damage [66]. Moreover, it is anticipated that sulfur-based proteins found in bacteria and phosphorus-containing chemicals in DNA will interact with AuNPs to affect the respiratory chain, encourage cell division, and finally cause cell death. Through oxidative stress induction, limiting the production of biofilms, and cell membrane disruption, the AuNPs may also suppress or eliminate the pathogenic bacteria [67].

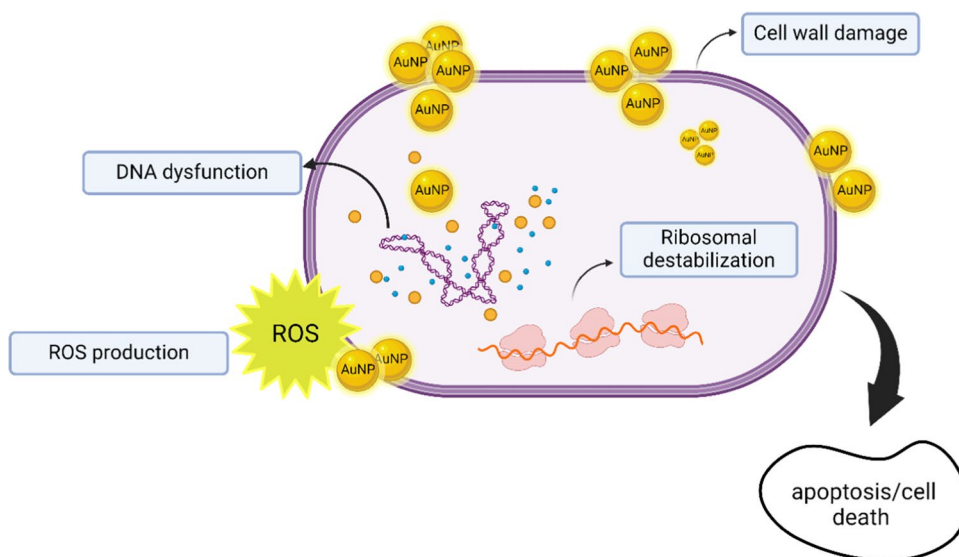
Nanomaterials have been shown to be a promising material with a wide range of real-world applications. The results of this experiment demonstrated that the extract obtained

from the leaves of *C. alata* acted as a successful reducing and capping agent during the production of AuNPs. By adhering to green chemistry principles, the synthesis technique did not utilize any harmful substances during the procedure. The nanoparticles showed remarkable stability and good physical properties. When tested against a few different bacteria, the generated nanoparticles showed strong antibacterial activity. The biological effects of AuNPs reduce inflammation and free radicals. The findings show that AuNPs that have been green-produced are a valuable natural resource with a variety of uses. Even though the green synthesis of AuNPs has advanced significantly, further study is required to boost trust in their safe and efficient application.

## 4 Conclusion

Using the extract from *C. alata* leaves, AuNPs were effectively produced. UV-Vis, TEM, EDS, zeta potential, and FTIR were used to validate the biosynthesized AuNPs' characteristics. Excellent antibacterial activity of AuNPs was shown against tested pathogenic microorganisms.

**Fig. 7** Mechanism of antibacterial action of AuNPs



Antioxidant and anti-inflammatory properties were also demonstrated by this nanoparticle.

**Acknowledgements** We would like to thank E-Layanan Sains (ELSA), BRIN, for the analytical instruments.

**Author contribution** Investigating, data curation, formal analysis, writing original draft: Vania C. Situmorang (V.C.S.), Sahrur Ramadhan (S.R.). Writing original draft, editing, formal analysis, review and editing: Tia Okselni (T.O.). Review and resource: Marissa Angelina (M.A.), Rizna Triana Dewi (R.T.D.). Writing original draft, editing, formal analysis, review and editing: Eldiza Puji Rahmi (E.D.P.). Formal analysis, visualization: Hikmat Hikmat (H.H.), Melati Septiyanti (M.S.). Conceptualization, methodology, writing original draft, supervision, data curation, project administration: Abdi Wira Septama (A.W.S.)

**Funding** The study was financially supported by Rumah Program Organisasi Riset Nanomaterial, National Research and Innovation Agency (BRIN), Republic Indonesia.

**Data availability** All data generated and analyzed during this study are included in this article.

## Declarations

**Ethical approval** Not applicable.

**Conflict of interest** The authors declare no competing interests.

## References

- Salem SS (2023) A mini review on green nanotechnology and its development in biological effects. Arch Microbiol 205:128. <https://doi.org/10.1007/s00203-023-03467-2>
- Said A, Abu-Elghait M, Atta HM, Salem SS (2024) Antibacterial activity of green synthesized silver nanoparticles using *Lawsonia inermis* against common pathogens from urinary tract infection. Appl Biochem Biotechnol 196:85–98. <https://doi.org/10.1007/s12010-023-04482-1>
- Andleeb A, Andleeb A, Asghar S et al (2021) A systematic review of biosynthesized metallic nanoparticles as a promising anti-cancer-strategy. Cancers (Basel) 13:1–22. <https://doi.org/10.3390/cancers13112818>
- Detoni MB, da Silva Bortoleti BT, Tomiotto-Pellissier F et al (2023) Biogenic silver nanoparticle exhibits schistosomicidal activity in vitro and reduces the parasitic burden in experimental schistosomiasis mansoni. Microbes Infect 25:1–13. <https://doi.org/10.1016/j.micinf.2023.105145>
- Abu-Elghait M, Soliman MKY, Azab MS, Salem SS (2023) Response surface methodology: optimization of myco-synthesized gold and silver nanoparticles by *Trichoderma saturnisporum*. Biomass Convers Biorefinery. <https://doi.org/10.1007/s13399-023-05188-4>
- Barabadi H, Mobaraki K, Jounaki K et al (2023) Exploring the biological application of *Penicillium fimorum*-derived silver nanoparticles: in vitro physicochemical, antifungal, biofilm inhibitory, antioxidant, anticoagulant, and thrombolytic performance. Heliyon 9:e16853. <https://doi.org/10.1016/j.heliyon.2023.e16853>
- Hosseini M, Mashreghi M, Eshghi H (2016) Biosynthesis and antibacterial activity of gold nanoparticles coated with reductase enzymes. Micro Nano Lett 11:484–489. <https://doi.org/10.1049/mnl.2016.0065>
- Bharadwaj KK, Rabha B, Pati S, et al (2021) Green synthesis of gold nanoparticles using plant extracts as beneficial prospect for cancer theranostics. Molecules 26. <https://doi.org/10.3390/molecules26216389>
- Marslin G, Siram K, Maqbool Q et al (2018) Secondary metabolites in the green synthesis of metallic nanoparticles. Materials (Basel) 11:1–25. <https://doi.org/10.3390/ma11060940>
- Mendez-Encinas MA, Valencia D, Ortega-García J, et al (2023) Anti-inflammatory potential of seasonal sonoran propolis extracts and some of their main constituents. Molecules 28. <https://doi.org/10.3390/molecules28114496>
- Thangamani N, Bhuvaneshwari N (2019) Green synthesis of gold nanoparticles using *Simarouba glauca* leaf extract and their biological activity of micro-organism. Chem Phys Lett 732:136587. <https://doi.org/10.1016/j.cpllett.2019.07.015>
- Soto KM, López-Romero JM, Mendoza S, et al (2023) Rapid and facile synthesis of gold nanoparticles with two Mexican medicinal plants and a comparison with traditional chemical synthesis. Mater Chem Phys 295. <https://doi.org/10.1016/j.matchemphys.2022.127109>
- Aljabali AAA, Akkam Y, Al Zoubi MS et al (2018) Synthesis of gold nanoparticles using leaf extract of *Ziziphus zizyphus* and their antimicrobial activity. Nanomaterials 8:1–15. <https://doi.org/10.3390/nano8030174>
- Satpathy S, Patra A, Ahirwar B, Hussain MD (2020) Process optimization for green synthesis of gold nanoparticles mediated by extract of *Hygrophila spinosa* T. Anders and their biological applications. Phys E Low-Dimensional Syst Nanostructures 121:113830. <https://doi.org/10.1016/j.physe.2019.113830>
- Hu X, Zhang Y, Ding T et al (2020) Multifunctional gold nanoparticles: a novel nanomaterial for various medical applications and biological activities. Front Bioeng Biotechnol 8:1–17. <https://doi.org/10.3389/fbioe.2020.00990>
- Fatmawati S, Yuliana PAS, Abu Bakar MF (2020) Chemical constituents, usage and pharmacological activity of *Cassia alata*. Heliyon 6:e04396. <https://doi.org/10.1016/j.heliyon.2020.e04396>
- Toh SC, Lihan S, Bunya SR, Leong SS, (2023) In vitro antimicrobial efficacy of *Cassia alata* (Linn.) leaves, stem, and root extracts against cellulitis causative agent *Staphylococcus aureus*. BMC Complement Med Ther 23:85. <https://doi.org/10.1186/s12906-023-03914-z>
- Oyedemi BO, Oyedemi SO, Chibuzor JV, et al (2018) Pharmacological evaluation of selected medicinal plants used in the management of oral and skin infections in Ebem-Ohafor District, Abia State, Nigeria. Sci World J 2018. <https://doi.org/10.1155/2018/4757458>
- Angelina M, Mardhiyah A, Dewi RT et al (2021) Physicochemical and phytochemical standardization, and antibacterial evaluation of *Cassia alata* leaves from different locations in Indonesia. Pharmacia 68:947–956. <https://doi.org/10.3897/PHARMACIA.68.E76835>
- Huq MA, Ashrafudoulla M, Rahman MM et al (2022) Green synthesis and potential antibacterial applications of bioactive silver nanoparticles: a review. Polymers (Basel) 14:742. <https://doi.org/10.3390/polym14040742>
- Paosen S, Billman S, Wunnoo S et al (2023) Control of biomaterial-associated infections through biofabrication of gold nanoparticles using *Musa sapientum* extract. Biotechnol J 18:1–39. <https://doi.org/10.1002/biot.202300008>
- Punnoose MS, Bijimol D, Mathew B (2021) Microwave assisted green synthesis of gold nanoparticles for catalytic degradation of environmental pollutants. Environ Nanotechnology, Monit Manag 16:100525. <https://doi.org/10.1016/j.enmm.2021.100525>
- Okselni T, Santoni A, Dharma A, Efdi M (2019) Biological activity of methanol extract of *Elaeocarpus mastersii* King:

- antioxidant, antibacterial, and  $\alpha$ -glucosidase inhibitor. *Rasayan J Chem* 12:146–151. <https://doi.org/10.31788/RJC.2019.1215019>
24. Moges A, Goud VV (2022) Optimization, characterization, and evaluation of antioxidant and antibacterial activities of silver nanoparticles synthesized from *Hippophae salicifolia* D. Don *Inorg Chem Commun* 146:110086. <https://doi.org/10.1016/j.inoche.2022.110086>
  25. Nirmal NP, Panichayupakaranant P (2015) Antioxidant, antibacterial, and anti-inflammatory activities of standardized brazilin-rich *Caesalpinia sappan* extract. *Pharm Biol* 53:1339–1343. <https://doi.org/10.3109/13880209.2014.982295>
  26. Septama AW, Tasfityati AN, Kristiana R, Jaisi A (2022) Chemical profiles of essential oil from Javanese turmeric (*Curcuma xanthorrhiza* Roxb.), evaluation of its antibacterial and antibiofilm activities against selected clinical isolates. *South African J Bot* 146:728–734. <https://doi.org/10.1016/j.sajb.2021.12.017>
  27. Nguyen VP, Le Trung H, Nguyen TH et al (2021) Advancement of microwave-assisted biosynthesis for preparing Au nanoparticles using *Ganoderma lucidum* extract and evaluation of their catalytic reduction of 4-nitrophenol. *ACS Omega* 6:32198–32207. <https://doi.org/10.1021/acsomega.1c05033>
  28. Vorobyova V, Skiba M, Vinnichuk K, Vasyliov G (2024) Synthesis of gold nanoparticles using plum waste extract with green solvents. *Sustain Chem Environ* 6:100086. <https://doi.org/10.1016/j.scenv.2024.100086>
  29. Al-Radadi NS (2021) Facile one-step green synthesis of gold nanoparticles (AuNp) using licorice root extract: antimicrobial and anticancer study against HepG2 cell line. *Arab J Chem* 14:102956. <https://doi.org/10.1016/j.arabjc.2020.102956>
  30. Aghamirzaei M, Khiabani MS, Hamishehkar H et al (2021) Antioxidant, antimicrobial and cytotoxic activities of biosynthesized gold nanoparticles (AuNPs) from Chinese lettuce (CL) leave extract (*Brassica rapa* var. *pekinensis*). *Mater Today Commun* 29:102831. <https://doi.org/10.1016/j.mtcomm.2021.102831>
  31. Patil TP, Vibhute AA, Patil SL et al (2023) Green synthesis of gold nanoparticles via *Capsicum annum* fruit extract: characterization, antiangiogenic, antioxidant and anti-inflammatory activities. *Appl Surf Sci Adv* 13:100372. <https://doi.org/10.1016/j.apsadv.2023.100372>
  32. Gaddam SA, Kotakadi VS, Sai Gopal DVR, et al (2014) Efficient and robust biofabrication of silver nanoparticles by *Cassia alata* leaf extract and their antimicrobial activity. *J Nanostructure Chem* 4. <https://doi.org/10.1007/s40097-014-0082-5>
  33. Happy A, Soumya M, Venkat Kumar S et al (2019) Phyto-assisted synthesis of zinc oxide nanoparticles using *Cassia alata* and its antibacterial activity against *Escherichia coli*. *Biochem Biophys Reports* 17:208–211. <https://doi.org/10.1016/j.bbrep.2019.01.002>
  34. Amini SM, Akbari A (2019) Metal nanoparticles synthesis through natural phenolic acids. *IET Nanobiotechnol* 13:771–777. <https://doi.org/10.1049/iet-nbt.2018.5386>
  35. Thanh NTK, Maclean N, Mahiddine S (2014) Mechanisms of nucleation and growth of nanoparticles in solution. *Chem Rev* 114:7610–7630. <https://doi.org/10.1021/cr400544s>
  36. Boruah JS, Devi C, Hazarika U et al (2021) Green synthesis of gold nanoparticles using an antiepileptic plant extract: in vitro biological and photo-catalytic activities. *RSC Adv* 11:28029–28041. <https://doi.org/10.1039/d1ra02669k>
  37. Al-Radadi NS, Al-Bishri WM, Salem NA, ElShebiney SA (2024) Plant-mediated green synthesis of gold nanoparticles using an aqueous extract of *Passiflora ligularis*, optimization, characterizations, and their neuroprotective effect on propionic acid-induced autism in Wistar rats. *Saudi Pharm J* 32:101921. <https://doi.org/10.1016/j.jsps.2023.101921>
  38. Malaikolundhan H, Moorkan G, Krishnamoorthi G et al (2020) Anticarcinogenic effect of gold nanoparticles synthesized from *Albizia lebbek* on HCT-116 colon cancer cell lines. *Artif Cells, Nanomedicine, Biotechnol* 48:1206–1213. <https://doi.org/10.1080/21691401.2020.1814313>
  39. Khan AU, Khan M, Malik N et al (2019) Recent progress of algae and blue-green algae-assisted synthesis of gold nanoparticles for various applications. *Bioprocess Biosyst Eng* 42:1–15. <https://doi.org/10.1007/s00449-018-2012-2>
  40. Akintelu SA, Yao B, Folorunso AS (2021) Bioremediation and pharmacological applications of gold nanoparticles synthesized from plant materials. *Heliyon* 7:e06591. <https://doi.org/10.1016/j.heliyon.2021.e06591>
  41. Ahmad T, Bustam MA, Irfan M et al (2019) Mechanistic investigation of phytochemicals involved in green synthesis of gold nanoparticles using aqueous *Elaeis guineensis* leaves extract: role of phenolic compounds and flavonoids. *Biotechnol Appl Biochem* 66:698–708. <https://doi.org/10.1002/bab.1787>
  42. López-Miranda JL, Esparza R, Rosas G et al (2019) Catalytic and antibacterial properties of gold nanoparticles synthesized by a green approach for bioremediation applications. *3 Biotech* 9:1–9. <https://doi.org/10.1007/s13205-019-1666-z>
  43. Kim H seok, Seo YS, Kim K, et al (2016) Concentration effect of reducing agents on green synthesis of gold nanoparticles: size, morphology, and growth mechanism. *Nanoscale Res Lett* 11. <https://doi.org/10.1186/s11671-016-1393-x>
  44. Filippov SK, Khusnutdinov R, Murmiliuk A et al (2023) Dynamic light scattering and transmission electron microscopy in drug delivery: a roadmap for correct characterization of nanoparticles and interpretation of results. *Mater Horizons* 10:5354–5370. <https://doi.org/10.1039/d3mh00717k>
  45. Oliveira AEF, Pereira AC, Resende MAC, Ferreira LF (2023) Gold nanoparticles: a didactic step-by-step of the synthesis using the turkevich method, mechanisms, and characterizations. *Analytica* 4:250–263. <https://doi.org/10.3390/analytica4020020>
  46. Ramakrishna M, Rajesh Babu D, Gengan RM et al (2016) Green synthesis of gold nanoparticles using marine algae and evaluation of their catalytic activity. *J Nanostructure Chem* 6:1–13. <https://doi.org/10.1007/s40097-015-0173-y>
  47. Bhattacharjee S (2016) DLS and zeta potential - what they are and what they are not? *J Control Release* 235:337–351. <https://doi.org/10.1016/j.jconrel.2016.06.017>
  48. Singh P, Pandit S, Beshay M et al (2018) Anti-biofilm effects of gold and silver nanoparticles synthesized by the *Rhodiola rosea* rhizome extracts. *Artif Cells Nanomedicine Biotechnol* 46:886–899. <https://doi.org/10.1080/21691401.2018.1518909>
  49. Singh P, Mijakovic I (2022) Green synthesis and antibacterial applications of gold and silver nanoparticles from *Ligustrum vulgare* berries. *Sci Rep* 12:7902. <https://doi.org/10.1038/s41598-022-11811-7>
  50. Stozhko NY, Bukharinova MA, Khamzina EI, et al (2019) The effect of the antioxidant activity of plant extracts on the properties of gold nanoparticles. *Nanomaterials* 9. <https://doi.org/10.3390/nano9121655>
  51. Scherer R, Godoy HT (2009) Antioxidant activity index (AAI) by the 2,2-diphenyl-1-picrylhydrazyl method. *Food Chem* 112:654–658. <https://doi.org/10.1016/j.foodchem.2008.06.026>
  52. Kiran MS, Rajith Kumar CR, Shwetha UR et al (2021) Green synthesis and characterization of gold nanoparticles from *Moringa oleifera* leaves and assessment of antioxidant, antidiabetic and anticancer properties. *Chem Data Collect* 33:100714. <https://doi.org/10.1016/j.cdc.2021.100714>
  53. Bhakya S, Muthukrishnan S, Sukumaran M, Muthukumar M (2016) Biogenic synthesis of silver nanoparticles and their antioxidant and antibacterial activity. *Appl Nanosci* 6:755–766. <https://doi.org/10.1007/s13204-015-0473-z>
  54. Zeb A (2020) Concept, mechanism, and applications of phenolic antioxidants in foods. *J Food Biochem* 44:1–22. <https://doi.org/10.1111/jfbc.13394>

55. Donga S, Bhadu GR, Chanda S (2020) Antimicrobial, antioxidant and anticancer activities of gold nanoparticles green synthesized using *Mangifera indica* seed aqueous extract. *Artif Cells, Nanomedicine Biotechnol* 48:1315–1325. <https://doi.org/10.1080/21691401.2020.1843470>
56. Sivakavinesan M, Vanaja M, Lateef R et al (2022) *Citrus limetta* Risso peel mediated green synthesis of gold nanoparticles and its antioxidant and catalytic activity. *J King Saud Univ Sci* 34:102235. <https://doi.org/10.1016/j.jksus.2022.102235>
57. Varghese BA, Nair RVR, Jude S et al (2021) Green synthesis of gold nanoparticles using *Kaempferia parviflora* rhizome extract and their characterization and application as an antimicrobial, antioxidant and catalytic degradation agent. *J Taiwan Inst Chem Eng* 126:166–172. <https://doi.org/10.1016/j.jtice.2021.07.016>
58. Gopalakrishnan V, Singaravelan R (2023) Enhanced antidiabetic and antioxidant properties of gold nanoparticles green synthesized using blossom extract of *Azadirachta indica*: in vitro studies. *Inorg Chem Commun* 158:111609. <https://doi.org/10.1016/j.inoche.2023.111609>
59. Dhayalan M, Denison MIJ, Anitha Jegadeeshwari L et al (2017) In vitro antioxidant, antimicrobial, cytotoxic potential of gold and silver nanoparticles prepared using *Embelia ribes*. *Nat Prod Res* 31:465–468. <https://doi.org/10.1080/14786419.2016.1166499>
60. Uzma M, Prasad DR, Sunayana N et al (2021) Studies of in vitro antioxidant and anti-inflammatory activities of gold nanoparticles biosynthesized from a medicinal plant, *Commiphora wightii*. *Mater Technol* 00:1–11. <https://doi.org/10.1080/10667857.2021.1905206>
61. Muniyappan N, Pandeewaran M, Amalraj A (2021) Green synthesis of gold nanoparticles using *Curcuma pseudomontana* isolated curcumin: its characterization, antimicrobial, antioxidant and anti-inflammatory activities. *Environ Chem Ecotoxicol* 3:117–124. <https://doi.org/10.1016/j.enceco.2021.01.002>
62. Khuda F, Ul Haq Z, Ilahi I et al (2021) Synthesis of gold nanoparticles using *Sambucus wightiana* extract and investigation of its antimicrobial, anti-inflammatory, antioxidant and analgesic activities. *Arab J Chem* 14:103343. <https://doi.org/10.1016/j.arabjc.2021.103343>
63. Arief S, Nasution FW, Zuhadjri LA (2020) High antibacterial properties of green synthesized gold nanoparticles using *Uncaria gambir* Roxb. leaf extract and triethanolamine. *J Appl Pharm Sci* 10:124–130. <https://doi.org/10.7324/JAPS.2020.10814>
64. Suriyakala G, Sathiyaraj S, Babujanarthanam R et al (2022) Green synthesis of gold nanoparticles using *Jatropha integerrima* Jacq. flower extract and their antibacterial activity. *J King Saud Univ Sci* 34:101830. <https://doi.org/10.1016/j.jksus.2022.101830>
65. Timoszyk A, Grochowalska R (2022) Mechanism and antibacterial activity of gold nanoparticles (AuNPs) functionalized with natural compounds from plants. *Pharmaceutics* 14:2599. <https://doi.org/10.3390/pharmaceutics14122599>
66. Dayem AA, Hossain MK, Bin LS et al (2017) The role of reactive oxygen species (ROS) in the biological activities of metallic nanoparticles. *Int J Mol Sci* 18:120. <https://doi.org/10.3390/ijms18010120>
67. Baptista PV, McCusker MP, Carvalho A et al (2018) Nanostrategies to fight multidrug resistant bacteria—“A Battle of the Titans.” *Front Microbiol* 9:1–26. <https://doi.org/10.3389/fmicb.2018.01441>

**Publisher's note** Springer Nature remains neutral with regard to jurisdictional claims in published maps and institutional affiliations.

Springer Nature or its licensor (e.g. a society or other partner) holds exclusive rights to this article under a publishing agreement with the author(s) or other rightsholder(s); author self-archiving of the accepted manuscript version of this article is solely governed by the terms of such publishing agreement and applicable law.